ELSEVIER

Journal of Biomechanics 41 (2008) 2379–2387

JOURNAL OF BIOMECHANICS

www.elsevier.com/locate/jbiomech
www.JBiomech.com

A multi-modular tensegrity model of an actin stress fiber

Yaozhi Luo[a], Xian Xu[a], Tanmay Lele[b,c], Sanjay Kumar[b,d], Donald E. Ingber[b,e,*]

[a]*Department of Civil Engineering, College of Architecture and Civil Engineering, Zhejiang University, PR China*
[b]*Karp Family Research Laboratories, Departments of Pathology and Surgery, Vascular Biology Program, Children's Hospital and Harvard Medical School, 11.127,300 Longwood Avenue, Boston, MA 02115-5737, USA*
[c]*Department of Chemical Engineering, University of Florida, Gainesville, FL, USA*
[d]*Department of Bioengineering, University of California, Berkeley, CA, USA*
[e]*Harvard Institute for Biologically Inspired Engineering, Cambridge, MA, USA*

Accepted 26 May 2008

Abstract

Stress fibers are contractile bundles in the cytoskeleton that stabilize cell structure by exerting traction forces on the extracellular matrix. Individual stress fibers are molecular bundles composed of parallel actin and myosin filaments linked by various actin-binding proteins, which are organized end-on-end in a sarcomere-like pattern within an elongated three-dimensional network. While measurements of single stress fibers in living cells show that they behave like tensed viscoelastic fibers, precisely how this mechanical behavior arises from this complex supramolecular arrangement of protein components remains unclear. Here we show that computationally modeling a stress fiber as a multi-modular tensegrity network can predict several key behaviors of stress fibers measured in living cells, including viscoelastic retraction, fiber splaying after severing, non-uniform contraction, and elliptical strain of a puncture wound within the fiber. The tensegrity model can also explain how they simultaneously experience passive tension and generate active contraction forces; in contrast, a tensed cable net model predicts some, but not all, of these properties. Thus, tensegrity models may provide a useful link between molecular and cellular scale mechanical behaviors and represent a new handle on multi-scale modeling of living materials.

Keywords: Cell mechanics; Cell structure; Computer model; Contractility; Cytoskeleton; Tensegrity

1. Introduction

Cultured cells exert traction on the extracellular matrix (ECM) by assembling cytoskeletal stress fiber (SF) bundles that extend tens of micrometers in length and insert into adhesion complexes at the cell–ECM interface. SFs are linear bundles of parallel actin and myosin filaments that also contain other actin-binding linker proteins, including tropomyosin, troponin, α-actinin and caldesmon. These components self-assemble into a periodic three-dimensional (3D) lattice reminiscent of the sarcomeric arrangement of thin and thick filaments in muscle (Langanger et al., 1986). These multi-molecular assemblies have been shown to shorten and generate tension in intact living cells (Kumar et al., 2006), membrane-permeabilized cells (Kreis and Birchmeier, 1980; Sims et al., 1992), and when isolated (Katoh et al., 1998, 2001a). Cell-generated tensional forces drive changes in cell shape and ECM remodeling, and contribute to the control of cell growth and function, as well as tissue patterning and mechanotransduction at the organ level (Ingber, 2003, 2006). Yet, little is known about how the supramolecular architecture of the SF contributes to its mechanical behavior.

Studies with isolated SFs reveal that they can shorten by ~20% (Katoh et al., 1998) in response to agonists that induce contraction in membrane-permeabilized cells (Sims et al., 1992). This observation, combined with the finding that SFs shorten ~15% within 1 s after being dislodged

*Corresponding author at: Karp Family Research Laboratories, Departments of Pathology and Surgery, Vascular Biology Program, Children's Hospital and Harvard Medical School, 11.127 300 Longwood Avenue, Boston, MA 02115-5737, USA.
Tel.: +1 617 919 2223; fax: +1 617 730 0230.
E-mail address: donald.ingber@childrens.harvard.edu (D.E. Ingber).

0021-9290/$ - see front matter © 2008 Elsevier Ltd. All rights reserved.
doi:10.1016/j.jbiomech.2008.05.026

from their ECM adhesions in lysed cells, has led to the conclusion that SFs are passively strained by ~20% (Kumar et al., 2006). When intact SFs were physically severed with femtosecond laser in living cells adherent to ECM, they retracted on the time scale of 15–20 s with viscoelastic recoil dynamics, and most of this response could be inhibited by interfering with myosin-based contractility (Kumar et al., 2006). These results indicate that the tension experienced by the SF is primarily due to active tension generation; however, even under these conditions, there was a small contribution of passive tension to SF retraction. Thus, SFs are both passively distended through their ECM attachments and actively tensed by internal myosin motors.

Other experiments show that SFs buckle in cells adherent to tensed flexible substrates when tension is released and the substrate retracts rapidly (Costa et al., 2002). These findings suggest that SFs experienced a non-uniform distribution of ~0–20% pre-extension, and that they can resist compression even though they also actively contract and shorten. Moreover, SFs do not significantly change their width when they contract against fixed adhesions (Kumar et al., 2006), and hence some of their components must resist lateral compression exerted by neighboring actomyosin filaments. It is therefore difficult to envision how SFs can be organized at the molecular level to provide this unique combination of mechanical properties.

Individual SFs in living cells behave mechanically like tensed viscoelastic cables, and their recoil dynamics can be captured by a macroscopic, continuum model that incorporates springs and dashpots (Kumar et al., 2006). Yet, the reality is that each SF is organized as a discrete 3D network composed of multiple interacting fibrillar components. Thus, there is a need for physical models that incorporate the discrete nature of these molecular building components and quantitatively relate component properties to network behavior.

Discrete network models based on tensegrity architecture have been used to successfully predict the mechanical responses of whole cells (Ingber, 1993, 2003; Wang et al., 1993; Stamenovic et al., 1996; Stamenovic and Coughlin, 2000; Stamenovic and Ingber, 2002; Coughlin and Stamenovic, 1997; Volokh et al., 2000; Adasnwz et al., 2002; Sultan et al., 2004), the erythrocyte membrane (Vera et al., 2005) and viruses (Sitharam and Agbandje-Mckenna, 2006); they also have been studied for use as 'intelligent' materials and structures for commercial applications (Shea et al., 2002; Sultan and Skelton, 2003). Here we describe a mechanical model of an SF based on tensegrity, and show that this model effectively predicts a diverse range of SF behaviors observed in living cells, whereas a tensed cable network model of similar architecture fails to predict all of these behaviors. These results suggest that SFs may be effectively described as tensegrity structures even though the precise molecular architectural details remain unknown.

2. Method and model

2.1. Tensegrity model

Tensegrities are tensile network structures that require prestress in their members before external load is applied to self-stabilize and resist shape distortion. When a tensegrity is subjected to a mechanical load, or the prestress magnitudes in its members are varied such that the structure is out of equilibrium, it adjusts its configuration and the prestress in its members to reach a new equilibrium state (Tibert and Pellegrino, 2003). Tensegrities exhibit many common mechanical behaviors regardless of their geometric arrangement (Sultan and Skelton, 2003; Sultan et al., 2004), and thus we modeled the SF using a generic, planar tensegrity mast composed of multiple similar structural modules (Fig. 1A) to simplify the mathematical analysis. To mimic the high slenderness ratio of the SF (~100 based on width and length of 100 nm and 10 μm, respectively), the tensegrity model is 6 modules wide and 251 modules long with a slenderness ratio of 42 (Fig. 1A). Each module is composed of 8 structural members organized in a prestressed tensegrity array in which tension cables form a continuous web that is balanced by compression struts (Fig. 1B,C); in each module, the relative dimensions of the structural element lengths, l_1:l_2:l_3 (Fig. 1C), are 1:2:2. An additional member (number 9) is added to the modules located at the ends of the tensegrity model to maintain the entire structure in a state of prestress (De Jager and Skelton, 2006). Cables are treated as viscoelastic Voight elements that support only tensile forces, whereas struts are modeled as linearly elastic elements under compression. (See Supplementary Information for their constitutive characteristics.)

At the reference (initial) state, tensile forces in the cables are balanced by the compression forces in the struts and by the model's fixed ends. A single actin filament has a Young's modulus E on the order of GPa and cross-sectional area A of ~10 nm^2 (Gittes et al., 1993; Holmes et al., 1990; Kabsch et al., 1990; Kojima et al., 1994). While there are essentially no corresponding values available for other SF proteins (e.g., myosin, tropomyosin and α-actinin), the linear stiffness of the myosin–actin bridge and titin are ~2 pN/nm (Huxley and Tideswell, 1996) and 1–4 pN/nm (Jeffrey and Wang, 2004), respectively, in muscle, whereas that of an isolated actin filament is ~44 pN/nm (Gittes et al., 1993; Holmes et al., 1990; Kabsch et al., 1990; Kojima et al., 1994). Here we assume that the average cross-sectional areas and lengths of the cross-linking proteins have the same magnitude as those of actin filaments, and their cross-sectional stiffness therefore will be similarly one order smaller. To generalize the model while maintaining this ratio, we simplified calculations by assuming the sectional stiffness of the longitudinal cables (corresponding to F-actin) and the cross-linking proteins to be 1 and 0.1 pN, respectively.

2.2. Prestress in the tensegrity model

Given the geometry and dimensions of the tensegrity SF model (Fig. 1), the self-stressed state of the plane structure was determined by equilibrium analysis as $1{:}2{:}3{:}4{:}5{:}6{:}7{:}8{:}9 = -0.3605{:}-0.3605{:}+0.3000{:}+0.3000{:}+0.5000{:}+0.5000{:}+0.2236{:}+0.2236{:}+0.2000$ (−, compression; +, tension). This represents the ratio of the internal stress of the various members shown in Fig. 1B, and it indicates that the whole structure will remain in equilibrium and self-stabilize itself under these internal stresses if the elements 1–9 all have internal forces proportional to these ratios.

The prestress introduced into the planar, multi-modular tensegrity array (Fig. 1A) is equilibrated in part by the structure itself, and in part by reaction forces due to the end constraints. The former contribution ('self-stress') keeps the structure in a stable state without end constraints, which is consistent with the observation that SFs remain stable when they are isolated from living cells (Katoh et al., 1998). The magnitude of the self-stress used in this study ($-0.0295553, -0.0295553, +0.0245915, +0.0245915, +0.0409859, +0.0409859, +0.0183294, +0.0183294$ and $+0.0163943$ pN) is proportional to the self-stressed state values described above. We also introduced an additional prestress of 0.2 pN into the longitudinal cables of the tensegrity SF model because stress fibers are passively strained by about 20% in cells (Kumar et al.,

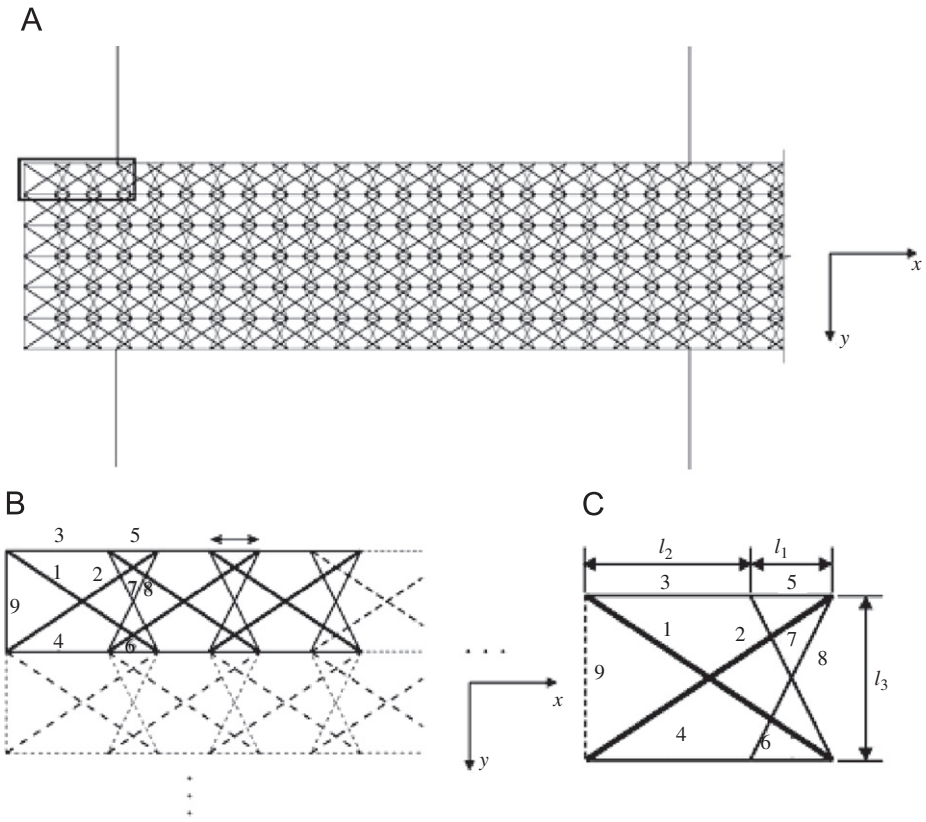

Fig. 1. Structural configuration of the multi-modular, tensegrity, SF model. (A) Organization of a large section of the planar multi-modular tensegrity the bold rectangle at the upper left indicates the area that is shown in greater detail in B. (B) Assembly of individual modules into a self-equilibrium tensegrity structure and (C) A single tensegrity module from A and B, with elements labeled: elements 1 and 2 (bold lines) are struts; 3–8 are cables (thin lines), and 9 (dashed line) is an additional cable for end modules. The modules connect one by one in the x-direction by overlapping by a distance of l_1, and they can be replicated in the y-direction by shifting a distance of l_2. Element 9 is only added to the distal ends of the modules of the model to mimic fixed ends of the SF and thereby, maintain structural self-equilibrium.

2006). Thus, in the presence of the self-equilibrated prestress, the tensegrity structure will remain in a state of static equilibrium without end constraints. In contrast, with passive prestress, the tensegrity structure will shorten if the end constraints are removed or relaxed (see Supplementary Information for details).

3. Results

While the precise molecular scale architecture of the SF is not known, we took advantage of the finding that tensegrity structures with different architectural configurations share common mechanical behaviors (Sultan and Skelton, 2003; Sultan et al., 2004), and used a generic tensegrity design in our model (Fig. 1). Our tensegrity SF model incorporates multiple linear filaments oriented in parallel along its main axis, with many lateral structural links that would correspond to actin-associated molecules (e.g., α-actinin, tropomyosin, troponin and caldesmon) that closely associate with actin and myosin filaments along their length (Burridge et al., 1988; Byers et al., 1984). We then used this simplified tensegrity model to explore whether it embodies features sufficient to predict mechanical behaviors previously observed in SFs in living cells.

3.1. Viscoelastic retraction and splaying of stress fibers

Past studies have demonstrated that individual SFs labeled with yellow fluorescent protein (YFP)-actin in living cells immediately retract when physically severed using a femtosecond laser and their cut ends splay (Fig. 2A) (Kumar et al., 2006). The dynamics of retraction closely match those exhibited by a tensed viscoelastic cable modeled using springs and dashpots (solid line, Fig. 2B). To explore whether the planar multi-modular tensegrity SF model exhibits similar viscoelastic retraction behavior, we modeled SF severing by deleting structural elements that span the width of the model at its center (Fig. 2C), and then carried out a structural transient analysis (ANSYS., 2004) that incorporates material damping of the cables. The predicted retraction kinetics of the tensegrity model were very sensitive to the viscoelastic characteristics of the cables, and matched experimentally observed kinetics for a material damping coefficient of 3 s/nm (Fig. 2B); this value was chosen for the rest of the simulations. Reducing the passive prestress of the model SF from 0.2 to 0.1 and then to 0 pN resulted in a progressive decrease in the retraction response (Fig. 2D) that also closely paralleled the response

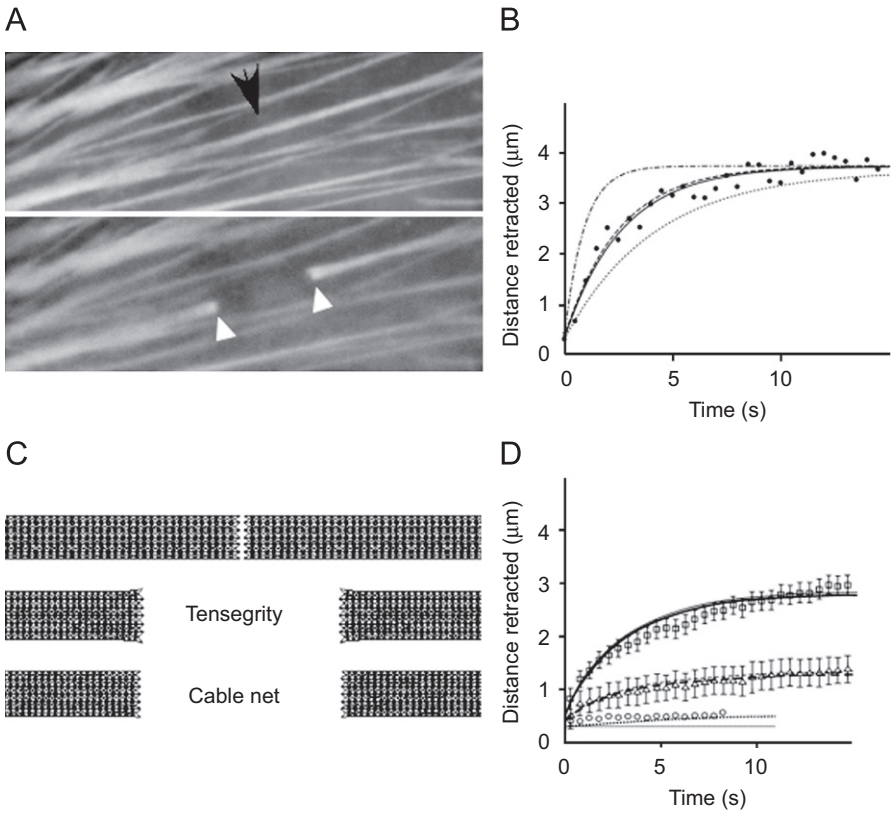

Fig. 2. SF retraction after surgical incision. (A) Fluorescence micrographs of a single YFP-labeled SF (arrow) before (top) and 15 s after (bottom) being surgically incised with a femtosecond laser (black arrow indicates site of laser irradiation; reprinted from (Kumar et al. (2006) with permission). Note that the cut ends of the SF (white arrowheads) physically retract and splay after cutting. (B) Time course of SF retraction predicted by the tensegrity model simulations with cable material damping coefficients of 5, 3 and 1 s/nm corresponding to time constants of 4.15 s (dashed–dotted line), 2.61 s (dashed line) and 0.9 s (dotted line), respectively. As can be seen, the simulation with a material damping coefficient of 3 s/nm matches the experimental data (black circles) and the predictions of a spring-dashpot model with a time constant of 2.66 s (solid line, Kumar et al., 2006). (C) Images showing results of simulations after the SF models are severed at their center (top). The tensegrity model both retracts and exhibits splayed ends (middle) like the living SF, whereas the purely tensed cable net model that lacks compression struts retracts but fails to produce similar splaying behavior (bottom). (D) Time course of SF retraction predicted by the tensegrity model simulation for a passive prestress of 0.2 pN (solid line), 0.1 pN (dashed line) or no passive prestress (dotted line) fit well to data obtained from experiments in which SFs were incised in control cells (squares) or treated with the chemical inhibitors of cytoskeletal tension generation, Y27632 (10 μM for 1 h) (triangles) or ML7 (67 μM for 30 min) (circles), respectively; error bars represent mean ± SEM.

exhibited by SFs in living cells when exposed to progressively more potent inhibitors of actomyosin-based tension generation (Y27632 or ML7, respectively; Kumar et al., 2006). Moreover, the cut ends of the tensegrity SF model also widened as the retraction distance increased, whereas a tensed cable model with identical structure to the tensegrity model (i.e., except lacking compression-resistant struts) did not exhibit any splaying response under identical loading conditions (Fig. 2C).

3.2. Stress fiber response to puncturing

When the laser was used to create a 300 nm wide puncture wound in a single living SF, the circular hole progressively deformed along the main axis of the SF due to internal prestress, resulting in the formation of an elliptical defect (Fig. 3A, top) (Kumar et al., 2006). In our simulations, when a hole was introduced into the tensegrity SF model, it also elongated and formed into an elliptical shape, but the SF narrowed along the lateral borders of the hole (not shown), whereas these regions maintained relatively constant in width in living cells (Fig. 3A, top). This subtle difference can be explained, however, if SFs have lateral constraints in addition to their end-links to fixed focal adhesions (Costa et al., 2002), as demonstrated by electron microscopy (Marek et al., 1982). We therefore incorporated lateral guy wires connected to the sides of the SF model to mimic these lateral flexible constraints in this and all subsequent modeling studies. Importantly, this tethered SF model effectively predicted the shape changes in the puncture wound observed in past experiments (Fig. 3A, bottom vs. top). Normalized values of simulated elongation measured during a time course of 15 s also closely matched the dynamic structural rearrangements observed in punctured SFs in living cells (Fig. 3B).

3.3. Stress fiber buckling

When tension is rapidly released in cells spread on stretched, flexible ECM substrates, the resulting cell

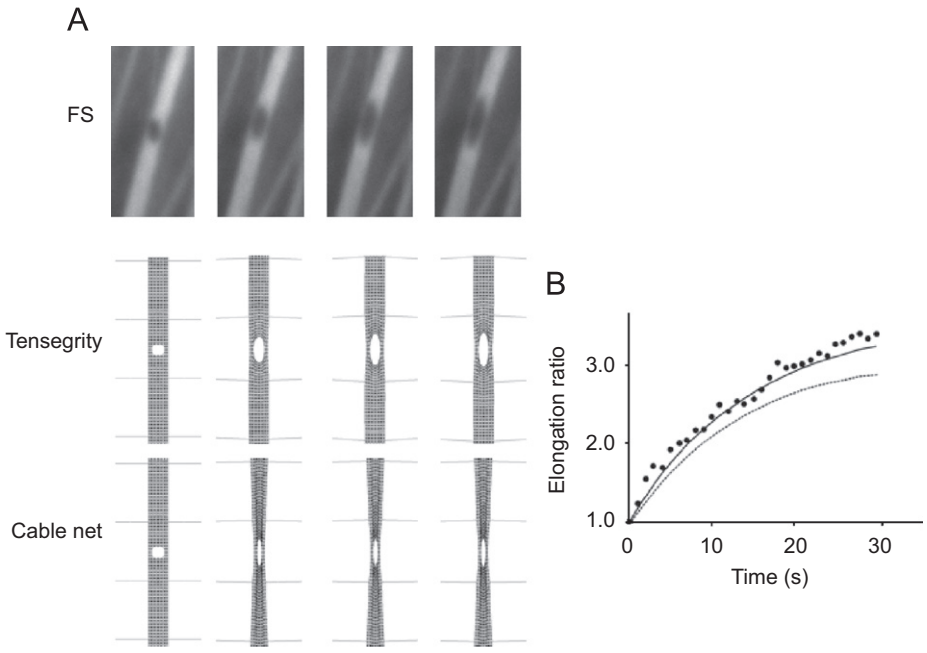

Fig. 3. Response of an SF to puncturing. (A) Progressive elongation of a puncture hole (300 nm diameter) produced in a YFP-labeled SF with a femtosecond laser (Kumar et al., 2006) over a period of 15 s (top), and analogous responses depicted in a computer simulation using the tensegrity SF model (middle) or a tensed cable net model (bottom). Note that only the tensegrity model mimics this SF behavior. (B) Graphic depiction of the time course of hole elongation along the main axis of the SF showing that the results of the tensegrity simulation (black line) fit well with previously reported experimental results (black circles; 5). In contrast, the rate of hole elongation exhibited by the cable net model (dashed line) was considerably slower than that displayed by SFs in living cells. The elongation ratio is defined as the ratio of increased diameter along the main axis to the initial diameter.

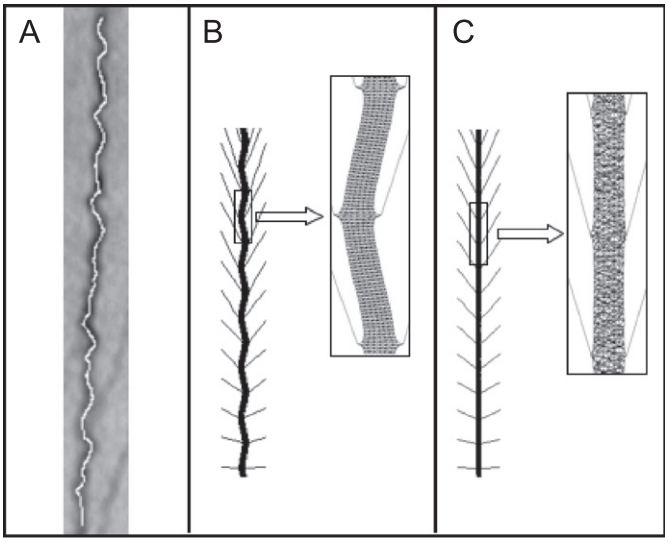

Fig. 4. Short-wave pattern of SF buckling. (A) Buckling pattern of an SF in living cells produced by rapid release of tension within cells adherent to stretched ECM substrates (reprinted with permission from Costa et al. (2002)) and (B) Periodic short wavelength buckling pattern produced in the tensegrity SF model (inset shows a portion of the buckled configuration at higher magnification). (C) A tensed cable net model does not buckle under similar shortening conditions. Enlarged view (inset) shows that the modules of this tensed net model become disorganized and no longer appear in register, which may indicate that its buckling was activated by the free motion of the structural members after loss of prestress.

retraction causes SFs aligned along the shortening direction to buckle when compressed rapidly beyond their unloaded slack length (Fig. 4A) (Costa et al., 2002). The pattern of buckling has a relatively short wavelength and varies along the length of the SF, which provides additional support for the existence of lateral constraints. A non-linear buckling analysis was carried out to determine the tensegrity model's response when one end was fixed and the other was subjected to a uniformly distributed compression force. These simulations revealed that the laterally tethered, multi-modular tensegrity SF also exhibited buckling behavior and short-wave wavelengths similar to that observed in living cells (Fig. 4B). Again, tethered tensile networks with the same architecture that lacked compression members failed to exhibit this behavior (Fig. 4C).

3.4. Non-uniform contraction of stress fibers

When cells containing SFs are treated with contractile agonists, many stress fibers do not contract uniformly along their lengths; instead, myosin activity preferentially concentrates at their ends, causing them to contract peripherally and stretch at their center (Peterson et al., 2004). SF contraction is driven by the relative motion of actin and myosin filaments along the main axis of the fiber, which increases internal isometric tension within the entire

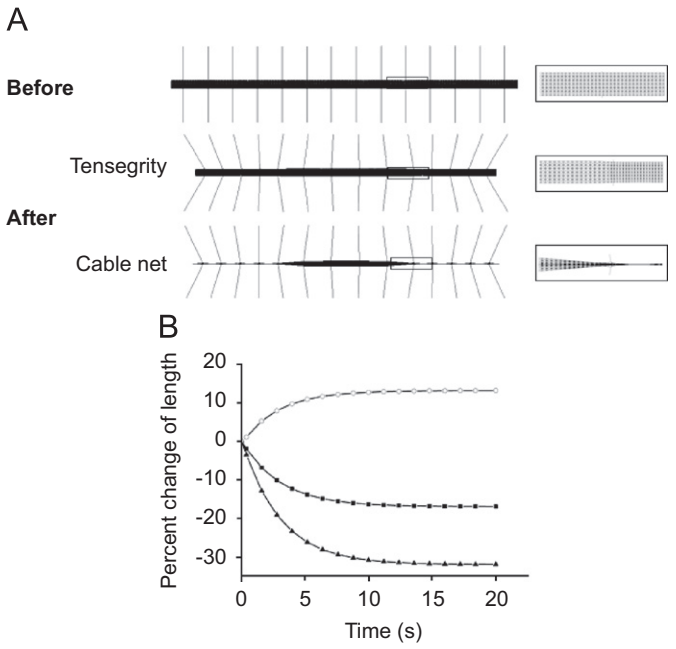

Fig. 5. (A) Configurations of the tensegrity SF model before (top) and after (middle) contraction, together with a comparable result from the tensed cable net model (bottom). Enlarged views of the junctions between the peripheral and central regions of the models pre- and post-contraction are shown in the insets at the right. (B) Graph showing the percentage change in length exhibited by the whole tensegrity SF (black squares) versus its peripheral (black triangles) and central regions (open circles).

fiber to the point where the total applied stress overcomes the stiffness of the SF (or subportions of it), as well as the resisting forces exerted by its anchoring points to basal focal adhesions. We therefore modeled this contraction as resulting from increased prestress in the SF.

A tensegrity SF model initially in a stable state of uniform pre-extension and flexibly fixed at its ends was divided into three parts: a central region surrounded by equally sized peripheral areas (Fig. 5A). Then the prestress of the longitudinal cables in the peripheral regions was increased to 0.8 pN to disturb the equilibrium. The structure rearranged its internal elements to find a new equilibrium state, resulting in contraction of the end portions of the tensegrity model, and stretching of its center (Fig. 5A,B). Thus, the tensegrity model qualitatively predicts the non-uniform contraction of SFs observed in living cells. In contrast, a cable net without compression struts did not capture this non-uniform retraction, and increasing the prestresses of all members resulted in uniform shortening of all elements in both models (data not shown).

Contraction of the tensegrity model resulted in 38% and 19% decreases in length of the peripheral regions and the whole SF, respectively (Fig. 5B), which are comparable to the magnitudes observed in living cells (Peterson et al., 2004). In contrast, the average elongation of the central region in the model was 18% (Fig. 5B), which is only one-third of the reported elongation of central sarcomeres in living SFs (Peterson et al., 2004). Interestingly, in our study, the whole tensegrity SF model shortened when contraction was increased (Fig. 5B), indicating that some prestress was released through the inward movement of the flexible fixed ends. In contrast, this would not occur in cells where the ends are fixed to stable ECM adhesions, and thus, increased elongation of the central region would result instead, as is observed experimentally.

3.5. Active contraction-dependent stress fiber shortening

SF shortening is due to actomyosin-based contraction; however, it is difficult to understand how a structure that behaves like a tensed viscoelastic cable and buckles when compressed can also actively contract and shorten. To investigate this further, we treated the compression struts in the tensegrity SF model as actuators whose lengths can be actively changed, as previously explored in studies of intelligent tensegrity structures for commercial applications (Shea et al., 2002; Sultan and Skelton, 2003).

To computationally mimic the stress and boundary conditions of the isolated SF (Katoh et al., 1998), we first anchored both ends of the tensegrity to a substrate and introduced prestress along its length (corresponding to its living state in a cell). Then, one of the ends was freed to release part of the prestress, resulting in passive retraction (as occurs during SF isolation). Finally, the struts were shortened in the simulation, thus mimicking active SF contraction due to actomyosin filament sliding. This caused all of the interconnected structural elements of the tensegrity network to rearrange and change their positions relative to each other, which caused the entire tensegrity model to shorten (Fig. 6A).

We quantified shortening of the tensegrity model by determining the ratio of the magnitude of the retraction to the initial length, as previously done with isolated SFs (Katoh et al., 1998). The stable configuration of the tensegrity SF before the struts were shortened was used as the reference state; convergent results were obtained when struts shortened to 20% of their initial length. In contrast to our studies on passive retraction, the width of the tensegrity SF model decreased with this active contraction (Fig. 6A), again predicting behavior of living SFs (Katoh et al., 1998). Due to the repeated multi-modular layout of the model, the normalized contraction scaled almost linearly with the normalized shortening of the struts (Fig. 6B). The corresponding contraction of the model only reached 10%, which was lower than the reported value of 23% (Katoh et al., 1998); however, by increasing strut stiffness from 0.1 to 0.2 pN (i.e., one fifth the stiffness of the longitudinal cables), we obtained convergent contraction of more than 30% with 40% strut shortening (Fig. 6B). This may indicate that cross-link elements in SFs are stiffer than we assumed, at least in the case of this particular tensegrity configuration.

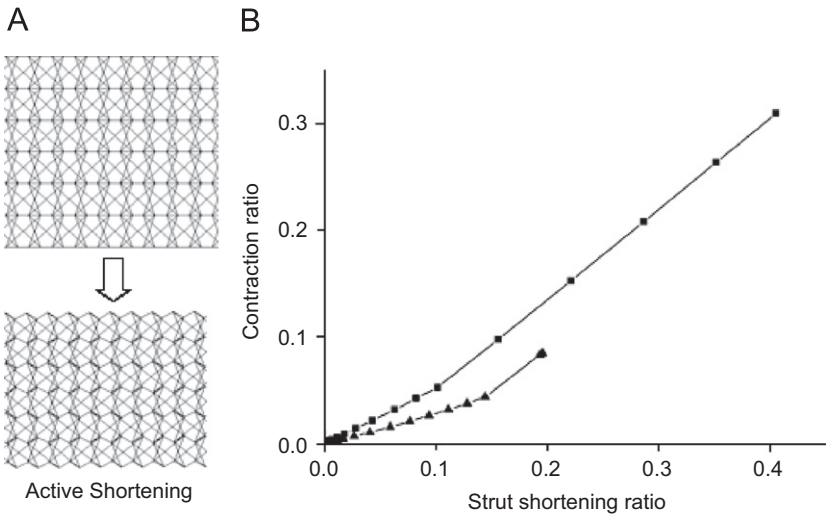

Fig. 6. Contraction response of the tensegrity SF model when struts are actively shortened. (A) The configurations of the model before (left) and after (right) struts are actively shortened showed that whole fiber contracts. (B) Graph showing SF contraction ratio as a function of strut shortening ratio for values of strut stiffness of 0.1 (triangle) or 0.2 (square); contraction and strut shortening were normalized by the initial length of the model and strut, respectively.

4. Discussion

Mechanical tension generated via actomyosin filament sliding within cytoskeletal SFs influences mammalian cell form and function, as well as tissue morphogenesis (Ingber, 2003, 2006). For this reason, the mechanical properties of SFs have been studied extensively both in vitro and in situ (Katoh et al., 1998, 2001b; Kreis and Birchmeier, 1980; Kumar et al., 2006; Sims et al., 1992). Yet, little is known about how the supramolecular architecture of the SF contributes to its wide range of novel mechanical behaviors, and a theoretical model to explain SF mechanics is lacking. Here, we developed and analyzed a generic, multi-modular tensegrity structure as a potential mechanical model of the SF, without attempting to mimic its precise molecular geometry at the nanoscale. Numerical simulations based on this multi-modular tensegrity effectively reproduced multiple physical behaviors of SFs that have been previously measured in living cells, including viscoelastic retraction and fiber splaying after severing, non-uniform contraction, buckling, and elliptical strain of a puncture hole created with a fine laser.

Importantly, the viscoelastic retraction of an SF can also be simulated by a single prestressed viscoelastic cable, but only the tensegrity model is capable of explaining all of these phenomena exhibited by SFs within living cells. In addition, tensed cable net structures with similar geometry, but lacking internal compression members, failed to mimic these behaviors. Without fixed ends (or a resisting compression strut), no prestress can be introduced into a cable net. As a result, if all of the elements of the SF are tensed, it will lose all prestress, become unstable after isolation, and exhibit no ability to contract, which is inconsistent with experimental observations (Katoh et al., 1998). In the tensegrity model, an increase in prestress also results in a more stable structure, and this result is consistent with the observation that highly phosphorylated myosin filaments, which are more contractile, are more rigid (Peterson et al., 2004). Thus, these observations suggest that the discrete network organization of the proteins in SFs should be taken into account in the investigation of their mechanical properties, and that at least a subset of these proteins may bear compression at the molecular scale in tensed SFs in living cells.

Although the precise organization of the SF remains to be determined, we can speculate that actin and myosin filaments function as tension cables, whereas some of the associated binding proteins (e.g., α-actinin, tropomyosin, troponin, caldesmon) act as lateral struts, either alone or in combination with actomyosin filaments, when the SF is in its tensionally prestressed state. These cross-linked filament bundles also resist compression and provide structural rigidity when tension is released, and this may contribute to SF buckling produced by rapid retraction of flexible substrates (Costa et al., 2002). Tropomyosin is a good candidate for a lateral strut as it significantly increases the stiffness of actomyosin filaments (Kojima et al., 1994), and it is absent from the more flexible hinge regions between sarcomeres and at the vertices of actin geodomes (Lazarides, 1976). The compression members in our tensegrity SF model are similarly distributed along the length of each repeating module, whereas they are relatively absent in the hinge regions between adjacent modules.

Regardless of the precise architecture, the use of a multi-modular tensegrity arrangement provides a mechanism to maintain and control self-equilibrium within subregions of the SF (e.g., center vs. periphery). It also provides similar functions at higher hierarchical levels, including at the level of the whole integrated SF, and the entire cell that contains multiple SFs that pull isometrically against fixed ECM

adhesions. If all the prestress in the SF were to equilibrate itself, no force interactions between SFs and the focal adhesions would occur. Thus, given that traction forces can be visualized at focal adhesions (Beningo et al., 2001), the prestress of each SF does appear to be balanced in part by the ability of their fixed ends to bear these loads.

It was recently reported that the Young's modulus of isolated SFs is ~1.45 MPa, which is some three orders of magnitude smaller than previously reported elastic moduli for single actin filaments (Deguchi et al., 2006). This difference may indicate that axial deformation of SFs is not simply caused by axial elongation/contraction of F-actins. Other mechanisms, such as tightening or relaxation of the mutual twisting of microfilament bundles, may also contribute to the axial deformation of SFs. While the relatively simple tensegrity model presented here does not incorporate these structural details, more sophisticated multi-modular tensegrity models may be able to do so. A key challenge in developing these models will be transitioning from planar 2D structures to more complex 3D geometries (along with more sophisticated algebraic formalisms) that will be needed to capture complex interfilament rearrangements.

A multi-modular tensegrity model of icosahedral shells has been used to explain the movement and self-assemblies of viral capsids (Sitharam and Agbandje-Mckenna, 2006), and viral self-assembly was also modeled based on icosahedral tensegrity using computational algebra (Caspar, 1980). Although virus assembly and SF contraction are two different physiological phenomena, their tensegrity models share a common mathematical basis, i.e. a 'form-finding' process in which the structure takes on a configuration with minimum potential energy under given constraints. In past studies, simple (single module) tensegrity models were shown to predict static and dynamic mechanical behaviors of living mammalian cells, including linear stiffening and instantaneous softening, elastic and viscoelastic characteristics, and cell shape modulation (Ingber, 1993, 2003; Wang et al., 1993; Stamenovic et al., 1996, Stamenovic and Coughlin, 2000; Stamenovic and Ingber, 2002; Coughlin and Stamenovic, 1997; Volokh et al., 2000; Adasnwz et al., 2002; Sultan et al., 2004). However, the tensegrity module used in most of those studies only has six compression members and 24 tension cables, and it fails to take into account the multi-modularity and structural hierarchies that are present in living cells (Ingber, 2003). For example, one SF may be severed in a cell adherent to a rigid substrate without fully compromising cell structure, whereas global structural rearrangements are observed throughout the cytoskeleton if these cells are attached to flexible ECM substrates (Kumar et al., 2006). The actin filaments that permeate the cytoplasm also display multiple levels of organization in that they can be organized as nets, geodesic dome-like structures, short bundles and long SFs, and actin-binding proteins can also organize into modular structures (Puius et al., 1998). Thus, the multi-modular tensegrity model presented here may offer more utility for simulating complex collective behaviors of these cellular components.

In summary, these studies suggest that the discrete network organization of the SF contributes greatly to its mechanical properties, and tensegrity principles convey multiple physical properties to these complex nanoscale structures in living cells. Although SFs are tensed, all of their subcomponents do not experience tension, and some of these elements must bear compressive forces at the molecular scale for the entire SF to exhibit its novel organic properties. Given that tensegrity appears to be utilized at multiple size scales in the hierarchy of life (Ingber, 2003, 2006), the multi-modular tensegrity model described here may provide a useful link between molecular and cellular scale mechanical behaviors, and provide a new handle with which to develop novel multi-scale models of living materials.

Conflict of interest statement

Please note that none of the authors of this paper have any financial and personal relationships with other people or organizations that could inappropriately influence (bias) the presented work.

Acknowledgments

This work was supported by grants from NIH (CA45548 and F32-NS048669), NSF (DMR-0213805 and MRSEC at Harvard University) and AHA 0735203N, and by a Pao Yu-Kong and Pao Zhao-Long Scholarship from Zhejiang University.

Appendix A. Supporting Information

Supplementary data associated with this article can be found in the online version at doi:10.1016/j.jbiomech.2008.05.026.

References

Adasnwz, P.C., Laurentz, V.M., Oddouw, C., Isabeyz, D., Wendlingw, S., 2002. A cellular tensegrity model to analyse the structural viscoelasticity of the cytoskeleton. Journal of Theoretical Biology 218, 155–173.

ANSYS., 2004. ANSYS Multiphysics, Canonsburg, PA.

Beningo, K.A., Dembo, M., Kaverina, I., Small, J.V., Wang, Y., 2001. Nascent focal adhesions are responsible for the generation of strong propulsive forces in migrating fibroblasts. The Journal of Cell Biology 153, 881–888.

Burridge, K., Fath, K., Kelly, K., Nuckolls, G., Turner, C., 1988. Focal adhesions: transmembrane junction between the extracellular matrix and the cytoskeleton. Annual Review of Cell Biology 4, 487–525.

Byers, H.R., White, G.E., Fujiwara, K., 1984. Organization and function of stress fibers in cells in vitro and in situ. Journal of Cell Muscle Motility 5, 83–137.

Caspar, D.L.D., 1980. Movement and self-control in protein assemblies. Biophysical Journal 32, 103–108.

Costa, K.D., Hucker, W.J., Yin, F.C., 2002. Buckling of actin stress fibers: a newwrinkle in the cytoskeletal tapestry. Cell Motility and the Cytoskeleton 52, 266–274.

Coughlin, M.F., Stamenovic, D., 1997. A tensegrity structure with buckling compression elements: application to cell mechanics. Journal of Applied Mechanics, ASME 64, 480–486.

Deguchi, S., Ohashi, T., Sato, M., 2006. Tensile properties of single stress fibers isolated from vascular smooth muscle cells. Journal of Biomechanics 39, 2603–2610.

De Jager, B., Skelton, R.E., 2006. Stiffness of planar tensegrity truss topologies. International Journal of Solids and Structures 43, 1308–1330.

Gittes, F., Mickey, B., Nettleton, J., Howard, J., 1993. Flexural rigidity of microtubules and actin filaments measured from thermal fluctuations in shape. Journal of Cell biology 120, 932–934.

Holmes, K.C., Popp, D., Gebhard, W., Kabsch, W., 1990. Atomic model of the actin filament. Nature 347, 44–49.

Huxley, A.F., Tideswell, S., 1996. Filament compliance and tensiontransients in muscle. Journal of Muscle Research and Cell Motility 17, 507–511.

Ingber, D.E., 1993. The riddle of morphogenesis: a question of solution chemistry or molecular cell engineering? Cell 75, 1249–1252.

Ingber, D.E., 2003. Tensegrity I. Cell structure and hierarchical systems biology. Journal of Cell Science 116, 1157–1173.

Ingber, D.E., 2006. Cellular mechanotransduction: putting all the pieces together again. FASEB Journal 20, 811–827.

Jeffrey, G.F., Wang, K., 2004. Simultaneous dynamic stiffness and extension profiles of single titin molecules: nanomechanical evidence for unfolding intermediates. Journal of Vacuum Science and Technology A: Vacuum, Surfaces, and Films 22, 1439–1444.

Kabsch, W., Mannherz, H.G., Suck, D., Pai, E.F., Holmes, K.C., 1990. Atomic structure of the actin:DNase I complex. Nature 347, 37–44.

Katoh, K., Kano, Y., Masuda, M., Onishi, H., Fujiwara, K., 1998. Isolation and contraction of the stress fiber. Molecular Biology of the Cell 9, 1919–1938.

Katoh, K., Kano, Y., Amano, M., Onishi, H., Kaibuchi, K., Fujiwara, K., 2001a. Rho-Kinase-mediated contraction of isolated stress fibers. Journal of Cell Biology 153, 569–583.

Katoh, K., Kano, Y., Amano, M., Kaibuchi, K., Fujiwara, K., 2001b. Stress fiber organization regulated by MLCK and Rho-kinase in cultured human fibroblasts. American Journal of Physiology Cell Physiology 280, 1669–1679.

Kojima, H., Ishijima, A., Yanagida, T., 1994. Direct measurement of stiffness of single actin filaments with and without tropomyosin by in vitro nanomanipulation. Proceedings of the National Academy of Sciences USA 91, 2962–12966.

Kreis, T.I., Birchmeier, W., 1980. Stress fiber sarcomers of fibroblasts are contractile. Cell 22, 555–561.

Kumar, S., Maxwell, I.Z., Heisterkamp, A., Polte, T.R., Lele, T., Salanga, M., Mazur, E., Ingber, D.E., 2006. Viscoelastic retraction of single living stress fibers and its impact on cell shape, cytoskeletal organization and extracellular matrix mechanics. Biophysical Journal 90, 3762–3773.

Langanger, G., Moeremans, M., Daneels, G., Sobieszek, A., De Brabander, M., De Mey, J., 1986. The molecular organization of myosin in stress fibers of cultured cells. Journal of Cell Biology 102, 200–209.

Lazarides, E., 1976. Actin, a-actinin, and tropomyosin interactions in the structural organization of actin filaments in nonmuscle cells. Journal of Cell Biology 68, 202–219.

Marek, L.F., Kelley, R.O., Perdue, B.D., 1982. Organization of the cytoskeleton in square fibroblasts. Cell Motility and the Cytoskeleton 2, 115–130.

Peterson, L.J., Rajfur, Z., Maddox, A.S., Freel, C.D., Chen, Y., Edlund, M., Otey, C., Burridge, K., 2004. Simultaneous stretching and contraction of stress fibers in vivo. Molecular Biology of the Cell 15, 3497–3508.

Puius, Y.A., Mahoney, N.M., Almo, S.C., 1998. The modular structure of actin-regulatory proteins. Current Opinion in Cell Biology 10, 23–34.

Shea, K., Fest, E., Smith, I.F.C., 2002. Developing intelligent tensegrity structures with stochastic search. Advanced Engineering Informatics 16, 21–40.

Sims, J., Karp, S., Ingber, D.E., 1992. Altering the cellular mechanical force balance results in integrated changes in cell, cytoskeletal and nuclear shape. Journal of Cell Science 103, 1215–1222.

Sitharam, M., Agbandje-Mckenna, M., 2006. Modeling virus self-assembly pathways: avoiding dynamics using geometric constraint decomposition. Journal of Computational Biology 13, 1232–1265.

Stamenovic, D., Coughlin, M.F., 2000. A quantitative model of cellular elasticity based on tensegrity. Journal of Biomechanical Engineering 122, 39–43.

Stamenovic, D., Ingber, D.E., 2002. Models of cytoskeletal mechanics of adherent cells. Biomechanics and Modeling in Mechanobiology 1, 95–108.

Stamenovic, D., Fredberg, J.J., Wang, N., Butler, J.P., Ingber, D.E., 1996. A microstructural approach to cytoskeletal mechanics based on tensegrity. Journal of Theoretical Biology 181, 125–136.

Sultan, C., Skelton, R., 2003. Deployment of tensegrity structures. International Journal of Solids and Structures 40, 4637–4657.

Sultan, C., Stamenovic, D., Ingber, D.E., 2004. A computational tensegrity model predicts dynamic rheological behaviors in living cells. Annals of Biomedical Engineering 32, 520–530.

Tibert, A.G., Pellegrino, S., 2003. Review of form-finding methods for tensegrity structures. International Journal of Space Structures 18, 209–223.

Vera, C., Skelton, R., Bossens, F., Sung, L.A., 2005. 3-D nanomechanics of an erythrocyte junctional complex in equibiaxial and anisotropic deformations. Annals of Biomedical Engineering 33, 1387–1404.

Volokh, K.Y., Vilnay, O., Belsky, M., 2000. Tensegrity architecture explains linear stiffening and predicts softening of living cells. Journal of biomechanics 33, 1543–1549.

Wang, N., Butler, J.P., Ingber, D.E., 1993. Mechanotransduction across the cell surface and through the cytoskeleton. Science 206, 1124–1127.